NEOPLASIA
www.neoplasia.com

Volume 14 Number 10 October 2012 pp. 952–963 952

Vitamin D Metabolism and Effects on Pluripotency Genes and Cell Differentiation in Testicular Germ Cell Tumors *In Vitro* and *In Vivo*[1,2]

Martin Blomberg Jensen*, Anne Jørgensen*, John Erik Nielsen*, Andreas Steinmeyer†, Henrik Leffers*, Anders Juul* and Ewa Rajpert-De Meyts*

*University Department of Growth and Reproduction, Rigshospitalet, Copenhagen, Denmark; †Bayer Schering Pharma AG, Berlin, Germany

Abstract

Testicular germ cell tumors (TGCTs) are classified as either seminomas or nonseminomas. Both tumors originate from carcinoma *in situ* (CIS) cells, which are derived from transformed fetal gonocytes. CIS, seminoma, and the undifferentiated embryonal carcinoma (EC) retain an embryonic phenotype and express pluripotency factors (NANOG/OCT4). Vitamin D (VD) is metabolized in the testes, and here, we examined VD metabolism in TGCT differentiation and pluripotency regulation. We established that the VD receptor (VDR) and VD-metabolizing enzymes are expressed in human fetal germ cells, CIS, and invasive TGCTs. VD metabolism diminished markedly during the malignant transformation from CIS to EC but was reestablished in differentiated components of nonseminomas, distinguished by coexpression of mesodermal markers and loss of OCT4. Subsequent *in vitro* studies confirmed that $1,25(OH)_2D_3$ (active VD) downregulated NANOG and OCT4 through genomic VDR activation in EC-derived NTera2 cells and, to a lesser extent, in seminoma-derived TCam-2 cells, and up-regulated brachyury, SNAI1, osteocalcin, osteopontin, and fibroblast growth factor 23. To test for a possible therapeutic effect *in vivo*, NTera2 cells were xenografted into nude mice and treated with $1,25(OH)_2D_3$, which induced down-regulation of pluripotency factors but caused no significant reduction of tumor growth. During NTera2 tumor formation, down-regulation of VDR was observed, resulting in limited responsiveness to cholecalciferol and $1,25(OH)_2D_3$ treatment *in vivo*. These novel findings show that VD metabolism is involved in the mesodermal transition during differentiation of cancer cells with embryonic stem cell characteristics, which points to a function for VD during early embryonic development and possibly in the pathogenesis of TGCTs.

Neoplasia (2012) 14, 952–963

Introduction

Testicular germ cell tumors (TGCTs) are a unique type of cancer because of their embryonic stem cell–like totipotentiality manifested by the ability to differentiate into all types of tissues. TGCTs comprise a heterogeneous group of neoplasms classified as either seminomas or nonseminomas, and both tumor types arise from preinvasive carcinoma *in situ* (CIS). CIS cells are thought to arise from abnormal fetal germ cells, presumably an arrested primordial germ cell or gonocyte. This notion is based on similar gene expression patterns, including expression of embryonic pluripotency factors and germ cell–specific genes [1]. After puberty, CIS cells begin to proliferate rapidly, undergo genomic aberrations, and develop invasive potential that facilitates tumor growth and development into an overt tumor [1–3]. The invasive seminoma retains a CIS-like phenotype and preserves expression of embryonic

Abbreviations: VD, vitamin D; TGCTs, testicular germ cell tumors; gla, osteocalcin

Address all correspondence to: Martin Blomberg Jensen, MD, University Department of Growth and Reproduction, Rigshospitalet, Section 5064, Blegdamsvej 9, DK-2100 Copenhagen, Denmark. E-mail: blombergjensen@gmail.com

[1]This work was supported by the Danish Cancer Society (E.R.D.M.), Villum Kann Rasmussen Foundation (A. Jø.), Lundbeck Foundation (E.R.D.M.), Rigshospitalet, and FSS: Danish Agency for Science, Technology and Innovation (M.B.J.). All authors state that they have no conflicts of interest.

[2]This article refers to supplementary materials, which are designated by Table W1 and Figures W1 to W5 and are available online at www.neoplasia.com.

Received 16 July 2012; Revised 27 August 2012; Accepted 28 August 2012

DOI 10.1593/neo.121164

markers, whereas the more aggressive nonseminoma is heterogeneous and subdivided histologically into undifferentiated embryonal carcinoma (EC), embryonic-like somatically differentiated teratoma, and the rare extraembryonally differentiated components (choriocarcinoma, yolk sac tumor) [4,5]. EC is characterized by an undifferentiated embryonic phenotype with expression of pluripotency factors such as NANOG, OCT4 (*POU5F1*), and SOX2, whereas teratomas, in which pluripotency factors are silenced, display an almost complete somatic differentiation mimicking embryonic development [2,6,7].

The transition from CIS to the formation of invasive tumors is poorly understood but may be influenced by chromosomal aberrations, e.g., amplification of the short arm of chromosome 12 (where *NANOG* and other pluripotency genes are localized), gene mutations, and constitutive activation of proteins (e.g., KIT). However, early intratubular testicular neoplasia is mainly composed of undifferentiated components and external factors may trigger further differentiation of the pluripotent EC components following invasion outside the seminiferous tubules [8]. Few factors can differentiate cancer cells to more mature phenotypes. Retinoic acid (RA) and vitamin D (VD) are potent differentiating agents in many mesodermal tissues [9,10], but VD has not previously been investigated for this ability in germ cells or testicular cancer.

VD is best known for its function in kidney, intestine, and bone. Inactive VD (cholecalciferol) is synthesized in the skin and hydroxylated by the hepatic 25-hydroxylases (CYP2R1 or CYP27A1) and the renal 1α-hydroxylase (CYP27B1) to the active $1,25(OH)_2D_3$ (calcitriol) that binds and activates the VD receptor (VDR) until inactivated by CYP24A1 [11]. VDR mediates either fast nongenomic effects or genomic effects through nuclear heterodimerization with RXR that enables binding to a VD response element in target genes and regulation of transcription [12]. In recent years, the spectrum for VD-mediated effects has expanded and comprises cell cycle control, suppression of proliferation, induction of cell cycle arrest, stimulation of apoptosis, and differentiation of normal and malignant cells [9,13,16]. VDR and VD-metabolizing enzymes are not exclusively expressed in the kidney but are also present in other mesodermal-derived tissues including adult male germ cells, as we and others have recently demonstrated [14,15]. Here, we investigated the expression of VDR and VD-metabolizing enzymes in a large series of TGCTs as well as in early fetal testes, where pluripotency genes are physiologically active in gonocytes. This was followed by mechanistic *in vitro* studies in three TGCT-derived cell lines, where $1,25(OH)_2D_3$ downregulated pluripotency genes and induced differentiation toward mesoderm. Finally, we tested the effects on tumor growth and pluripotency of low doses of cholecalciferol and $1,25(OH)_2D_3$ *in vivo* by using the EC-derived NTera2 cells in the nude mouse xenograft model.

Materials and Methods

Human Tissue Samples

Patients were recruited from the andrology clinic at Copenhagen University Hospital (Rigshospitalet, Denmark) in accordance with the Helsinki Declaration after approval from the local ethics committee (Permit No. KF 01 2006-3472). Adult testis samples were obtained from orchidectomy specimens performed because of TGCT. Tissue surrounding the tumor contained tubules with either CIS cells or normal/impaired spermatogenesis. Each sample was divided into fragments, which were either snap frozen and stored at −80°C for RNA extraction or fixed overnight at 4°C in formalin or paraformaldehyde and subsequently embedded in paraffin. An experienced pathologist evaluated all samples and immunohistochemical (IHC) markers were used for TGCT to ensure the histologic subtypes of the tumors. The number of tumor samples is given in Table 1. The fetal testicular tissue samples were obtained after induced or spontaneous abortions and stillbirths, mainly because of placental or maternal problems, and were formalin-fixed paraffin-embedded specimens from tissue archives at the Pathology Department (Rigshospitalet). Gestational age was calculated from the date of the last menstrual bleeding. Testes from seven fetuses, gestational weeks (GWs) 16, 18, 19, 20, 24, 32, and 39, were used for IHC studies.

Reverse Transcription–Polymerase Chain Reaction and Quantitative Reverse Transcription–Polymerase Chain Reaction Analysis

RNA was extracted from three classic seminomas (Sem), one mature teratoma, one embryonic carcinoma (EC), one mixed nonseminoma (EC, yolk sac, and choriocarcinoma), and five CIS samples (CIS adjacent to EC, Sem, mixed tumor, and two CIS from patients

Table 1. Expression of VDR and VD-Metabolizing Enzymes in TGCTs.

Histology	*N*	Activating Enzymes			Receptor VDR	Inactivating CYP24A1
		CYP2R1	CYP27A1	CYP27B1		
Germ cells (adult testis)	11–19	++ to +++ (19)	+ to +++ (11)	+ to ++ (14)	++ to +++ (12)	++ to +++ (14)
Fetal germ cells	7	ND	ND	ND	+ to ++ (7)	ND
CIS	11–17	None (17)	++ to +++ (11)	++ to +++ (13)	++ to +++ (13)	++ to +++ (13)
Seminoma	7–10	None to + (7)	+ (7)	+ to ++ (8)	+ to ++ (10)	+/– to ++ (9)
Nonseminoma						
EC	12–15	OCT4 pos., none OCT4 neg., +/– to + (15)	OCT4 pos., + to ++ OCT4 neg., +/– to + (12)	OCT4 pos., none to + OCT4 neg., + to ++ (12)	OCT4 pos., none to ++ OCT4 neg., + to +++ (14)	OCT4 pos., none to + OCT4 neg., + to +++ (12)
Teratoma	9–11	++ (10)	+ to ++ (11)	+ to +++ (9)	+ to +++ (9)	+ to +++ (10)
Yolk sac	4	None to +/– (4)	+ to ++ (4)	++ (4)	++ to +++ (4)	++ (4)
Choriocarc.	3	None to +/– (3)	+/– to + (3)	+ to ++ (3)	++ to +++ (3)	++ (3)
Subcellular localization		Cytoplasm	Cytoplasm	Cytoplasm	Cytoplasm/nuclear	Cytoplasm

Choriocarc, choriocarcinoma; ND, not determined.
(*x*) Corresponds to the number of samples investigated with the specific antibody.
The range of expression between the investigated samples is stated.
ECs are divided in OCT4-positive (OCT pos.) and OCT4-negative (OCT neg.) cells.

without an overt tumor). Normal testis RNA was also purchased from three different companies (Clontech-Takara Bio Europe, Paris, France; Abcam Plc, Cambridge, United Kingdom; and Biopharm US, Washington). RNA and cDNA preparation and reverse transcription–polymerase chain reaction (RT-PCR) were conducted as described previously [14,15]. RT-PCR was performed using specific primers targeting each mRNA (Table W1). Representative bands from each primer combination were sequenced for verification (Eurofins MWG GmbH, Ebersberg, Germany). Primers for *OCT4* and *NANOG* were designed to avoid known pseudogenes. Quantitative RT-PCR analysis was performed in triplicates using Stratagene Mx300P (Stratagene, La Jolla, CA) with SYBR Green QPCR Master Mix (Stratagene). Changes in gene expression were determined with the comparative C_T method using β2 microglobulin (β2M) as internal control (Table W1).

Immunohistochemistry

Primary antibodies were purchased from Santa Cruz Biotechnology Inc [Santa Cruz, CA; CYP2R1 (C-15; sc-48985), CYP27A1 (P-17; sc-14835), CYP27B1 (H-90; sc-67261), VDR (H-81; sc-9164), CYP24 (H-87; sc-66851), OCT4 (C-10; sc-5279), fibroblast growth factor 23 (FGF23; N-20; sc-16849), osteopontin (OPN; SPP1; lfmb-14; sc-73631), gla (BGLAP; FL-100; sc-30044)], SOX2 (AF 2018) from R&D Systems (Abingdon, UK), and Ki-67 (M7240), alpha-fetoprotein (AFP; A008), human chorionic gonadotropin (hCG; A0231) from DAKO (Glostrup, Denmark). The antibody against a germ cell antigen, MAGE-A4, was a kind gift from G. Spagnoli (University of Basel, Basel, Switzerland). VD-related antibodies were previously validated by IHC, *in situ* hybridization (ISH), and Western blot in human kidney samples and human spermatozoa [14,15]. The optimal dilutions of the primary antibodies in formalin-fixed reproductive tissue were CYP2R1, 1:100; CYP27A1, 1:200; CYP27B1, 1:200; VDR, 1:100; CYP24, 1:200; OCT4, 1:250; BGLAP (gla), 1:100; OPN, 1:100; FGF23, 1:200; SOX2, 1:200; KI-67, 1:100; AFP and hCG, 1:10,000; and MAGE, 1:250. The IHC and immunocytochemical (ICC) staining was performed according to a standard indirect peroxidase method as described previously [15]. Counterstaining was performed with Meyer hematoxylin. All experiments were performed with control staining without the primary antibody. Serial sections were used to examine concomitant expression of VDR and the VD-metabolizing enzymes with OCT4, SOX2, Ki-67, and BGLAP expression. Two independent investigators evaluated all slides and cytospins (M.B.J. and J.E.N.). Staining was classified according to an arbitrary semi-quantitative reference scale depending on the intensity of staining and the proportion of cells stained: +++, strong staining in nearly all cells; ++, moderate staining in the majority of cells; +, weak staining or a low percentage of cells stained; +/−, very weak staining in single cells; none, no positive cells detected. The proportion of positive cells was determined by counting 500 cells in a representative area.

Differentiation of Testicular Cell Lines

The EC-derived cell line NTera2 that is capable of differentiation along the neuroectodermal lineage after RA treatment, the EC-like 2102Ep with limited ability to differentiate [43], and the seminoma-derived TCam-2 cell line [44] were used in this study. Cells were grown under standard conditions at 37°C in 5% CO_2 atmosphere in Dulbecco's modified Eagle's medium (NTera2, 2102Ep) or RPMI 1640 (TCam-2) supplemented with glutamine (58.5 mg/ml), penicillin (100 U/ml), and streptomycin (100 mg/ml; all from Gibco, Naerum, Denmark). To investigate differentiation, we added $1,25(OH)_2D_3$ (1 nM to 10 μM), RA (10 μM), 25-hydroxyvitamin D_3 [$25(OH)D_3$; 100 nM to 1 μM], and the nuclear VDR antagonist ZK159222 (10 μM) to the media. DMSO was used as solvent, and all control samples were DMSO treated. Cells were plated in 25-cm^2 flasks and, every 48 hours, washed with phosphate-buffered saline and detached using 0.05% trypsin-EDTA for 5 minutes at 37°C, then half of the cells were plated in new 25-cm^2 flasks with new media and the other half were centrifuged down and the cell pellets were snap frozen for RNA purification. All chemicals were purchased from Sigma Aldrich (Brøndby, Denmark), except ZK 159222 that was obtained from Bayer Healthcare (Berlin, Germany).

Establishment of NTera2 Xenografts

All animal procedures were performed in compliance with the Danish Animal Experiments Inspectorate (License No. 2011/561-1956). A 6- to 8-week-old NMRI nude mice ($Fox1^{nu}$) were obtained from Taconic Europe (Ry, Denmark). Mice were housed and interventions were conducted at Pipeline Biotech in a designated pathogen-free area. European standard cages type 2 was used, and mice were fed Altromin 1324 *ad libitum* (600 IU cholecalciferol/kg; Altromin, Lage, Germany). NTera2 cells were treated with 100 nM $1,25(OH)_2D_3$ or vehicle for 20 days. Cells were grown under standard conditions and plated in 175-cm^2 flasks, and media were changed every 48 hours to replace $1,25(OH)_2D_3$. Matrigel was purchased from BD Biosciences (Albertslund, Denmark) and was diluted 1:2 in Dulbecco's modified Eagle's medium before mixing 1:1 with NTera2 cells. $1,25(OH)_2D_3$-treated NTera2 (5×10^6 cells) were injected subcutaneously into the right flank, and vehicle-treated NTera2 cells were injected subcutaneously to the left flank of male nude mice. Body weights and tumor volumes were measured three times weekly. Tumor volumes were calculated from two tumor diameter measurements using a vernier caliper: tumor volume = $L \times W \times 1/2W$. When the tumors reached about 150 mm^3 in size, the mice were randomized to the different treatment groups. The treatments were continued over a period of 4 weeks, although a maximal tumor diameter of 12 mm of one of the tumors necessitated earlier termination of animals.

Treatments

Seven animals received a diet fortified with cholecalciferol (1100 IU D_3/kg diet) from day 1, while the remaining 28 animals received standard diet (containing 600 IU D_3/kg diet). The 28 mice receiving standard diet were randomized into four different treatment groups 19 days after inoculation, including two control groups: 1) control group no treatment, received vehicle only (0.1% ethanol in sterile saline) three times weekly intraperitoneal (i.p.), 2) cisplatin control group for standard TGCT treatment, received 6 mg/kg i.v. once weekly, 3) calcitriol treatment group, received 0.05 μg of $1,25(OH)_2D_3$ i.p. three times weekly, and 4) cholecalciferol-fortified diet group (1100 IU D_3/kg diet) from day 19. At the end of the study, mice were killed according to animal welfare euthanasia statement. Tumors were harvested and weighed, and half were snap frozen in liquid nitrogen for RNA purification. The other half was fixed in formalin and embedded in paraffin for IHC.

Statistical Analysis

We used one-way analysis of variance and Bonferroni correction to test for variation between the treatment regimens in the xenograft

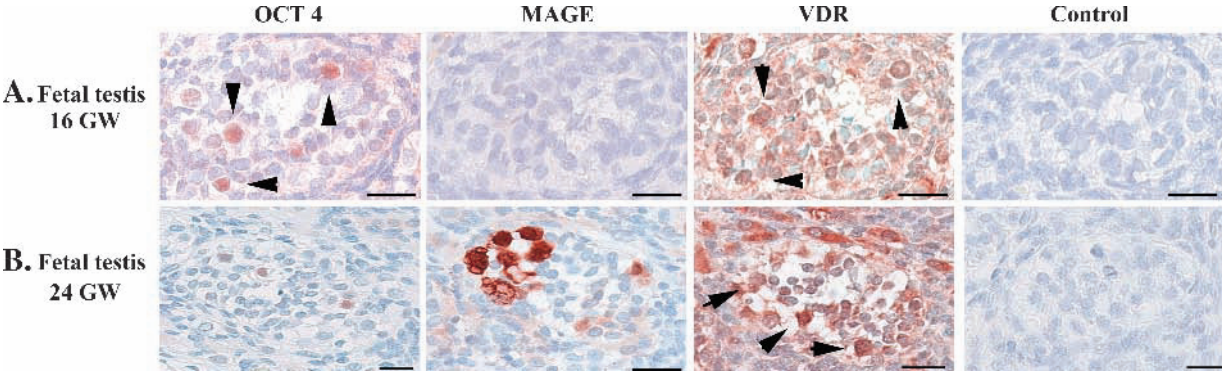

Figure 1. IHC expression of VDR in fetal germ cells. (A) IHC expression in serial sections from fetal testis 16 GW of OCT4, MAGE-A4, VDR, and negative control. (B) IHC from 24 GW. Arrowheads mark germ cells. Bar corresponds to 20 μm.

models. Differences in gene expression were tested by two-tailed Student's *t* test. $P < .05$ was considered statistically significant.

Results

VD Metabolism in Human Fetal Testis

The expression of the main components of the VD metabolism machinery was first investigated in fetal testes, where gonocytes, the presumptive precursors of CIS cells, are present. VDR was expressed in the nucleus and cytoplasm of fetal gonocytes (at GWs 16–20), identified by concomitant OCT4 expression and lack of MAGE-A4 expression (Figure 1*A*). VDR was also expressed in the nucleus and cytoplasm of fetal prespermatogonia (GWs 20–28), recognized by strong MAGE-A4 expression and lack of OCT4 (Figure 1*B*). Moreover, fetal Leydig cells had a marked cytoplasmic VDR expression, whereas approximately 40% of fetal Sertoli cells (GWs 16–28) expressed VDR in the nucleus and cytoplasm (Figure 1) unlike adult Sertoli cells, of which only a subset <5% expressed VDR (Figure 2*A*). In concert with the previously reported data [15], expression of *VDR* and all VD-metabolizing enzymes was detected on mRNA and protein level in all adult samples with normal spermatogenesis (Figures 2*A* and W1 and Table 1).

VD Metabolism in Testicular Germ Cell–Derived Neoplasms

CIS and seminoma. Transcripts of *VDR*, *CYP2R1*, *CYP27A1*, *CYP27B1*, and *CYP24A1* were detected in CIS and classic seminoma samples with varying intensity. In seminomas, *CYP2R1 mRNA* expression was high, whereas *CYP24A1* expression was low (Figure W1). There were no marked differences in the expression between the two pure CIS samples and the remaining CIS specimens adjacent to invasive TGCT (Figure W1). At the protein level, abundant cytoplasmic expression of VDR, CYP27A1, CYP27B1, and CYP24A1 was detected by IHC in >85% of CIS cells (Figure 2, *A* and *B*). However, CYP2R1 was not detected in the CIS cells and was absent or only weakly expressed in >80% of the investigated seminomas. CYP27A1 staining was also weak in seminomas, although 5% to 10% of the seminoma cells had an abundant CYP27A1 expression (Figure 2*C*). CYP27B1, VDR, and CYP24A1 were concomitantly expressed in the majority (>80%) of the seminoma cells characterized by nuclear OCT4 expression. The expression of CYP27B1 and CYP24A1 was weaker in seminomas than in CIS, and VDR was mainly expressed in the cytoplasm of CIS cells. By comparing staining intensity, the cytoplasmic VDR expression seemed stronger in CIS cells than in gonocytes (Figures 1*A* and 2, *A* and *B*). Interestingly, >70% seminoma cells expressed VDR in the nucleus, only 10% to 15% had a cytoplasmic VDR expression, and CYP24A1 was expressed in fewer seminoma cells than CYP27B1 and VDR (Figure 2*C*).

Nonseminomas. The differentiated somatic components of teratomas expressed most investigated transcripts, although *CYP27B1* was low and *CYP24A1* was undetectable in all nonseminomas (Figure W1). All the investigated proteins was found by IHC in most teratoma components, although the epithelial parts had none or low expression of CYP27B1 (Figure 2*E*). Mixed tumors containing differentiated syncytiotrophoblasts, choriocarcinoma, and undifferentiated EC had detectable transcripts of *CYP2R1*, *CYP27A1*, *CYP27B1*, and *VDR*, and the corresponding proteins were also detected in the cytoplasm of hCG-producing syncytiotrophoblasts and AFP-producing yolk sac components (Figures 2, *F* and *G*, and W1). The expression of VDR and VD-metabolizing enzymes tended to be mutually exclusive with OCT4 expression in the surrounding undifferentiated EC components (Figures 2, *D* and *E*, and W2).

CYP2R1 and *CYP27A1* transcripts were detected with low intensity in the undifferentiated EC, whereas *CYP27B1*, *VDR*, and *CYP24A1* transcripts were undetectable (Figure W1). IHC revealed that OCT4-positive parts of the nonseminomas had none or low expression of CYP27B1, VDR, and CYP24A1, whereas CYP27A1 was expressed in 10% to 15% of the EC cells (Figure 2, *D* and *E*). VD metabolism tended to be mutually exclusive with OCT4 expression. However, OCT4 expression was lower in the few EC cells that concomitantly expressed CYP27B1, CYP24A1, and VDR (predominantly cytoplasmic; Figures 2*E* and W2). In pure ECs and EC components of mixed nonseminomas, we noted morphologically aberrant EC cells expressing VDR and VD-metabolizing enzymes. These cells differed from classic EC cells as they appeared long and thin, had elongated nuclei and sparse elongated cytoplasm, and were OCT4-negative but expressed SOX2 (Figures 2*D*, W2, and W3). Serial sections revealed concomitant nuclear VDR expression with cytoplasmic osteocalcin expression in these EC cells, whereas osteocalcin (gla, BGLAP) expression was undetectable in the OCT4-positive EC cells (Figures W2 and W3).

VD Induces Differentiation of Cell Lines with Embryonic Stem Cell–Like Features

Two EC-like cell lines NTera2 and 2102Ep and the seminoma-like TCam-2 cell line that all express pluripotency factors were used

to test whether $1,25(OH)_2D_3$ (1–10 μM) induced differentiation. RA, known to differentiate human embryonic stem cell (hESC) and NTera2 cells, was used as positive control. RA (10 μM) downregulated *OCT4* and *NANOG* expression in both NTera2 and TCam-2 cells ($P < .001$; Figure 3). Both pluripotency factors were completely downregulated in NTera2 cells following RA treatment for 4 days, whereas the expression stabilized five-fold lower in TCam-2 cells after 6 days of treatment (Figure W4). The lower concentrations of $1,25(OH)_2D_3$ (1–10 nM) downregulated *OCT4* and *NANOG* significantly ($P < .01$) in NTera2 cells, whereas higher concentrations of $1,25(OH)_2D_3$ (>10 nM) abolished *OCT4* expression completely within 2 days in NTera2 cells and lowered *NANOG* expression 10-fold, unlike RA, which terminated *NANOG* expression completely (all $P < .001$; Figures 3 and W4). All the tested $1,25(OH)_2D_3$ concentrations were less potent than RA in the TCam-2 cells, in which $1,25(OH)_2D_3$ lowered *OCT4* expression

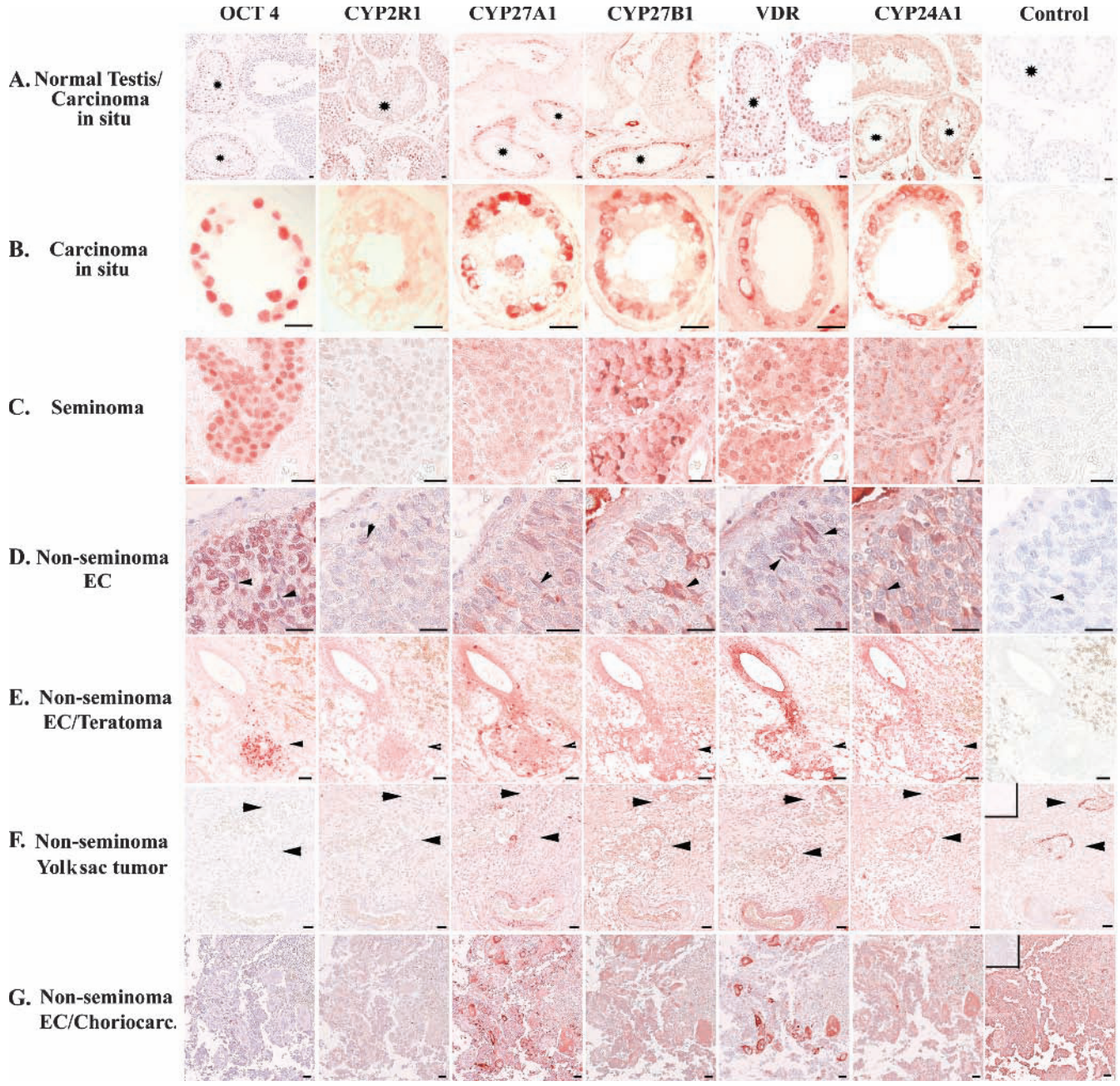

Figure 2. Expression of VDR and VD-metabolizing enzymes in normal testis and TGCTs. (A) IHC detection of proteins in normal and CIS tubules (marked with asterisk). (B) IHC expression in CIS with no counterstaining. (C) IHC expression in seminoma. (D) IHC expression in EC, arrowhead indicates OCT4-negative elongated EC cells. (E) IHC expression in mixed nonseminoma, arrowhead indicates OCT4-positive EC cells. (F) IHC expression in yolk sac tumor, arrowhead indicates α-fetoprotein–positive cells (positive control). (G) IHC expression in choriocarcinoma, and positive control shows hCG-producing cells. All control samples are negative control with no primary antibody and counterstained with Mayer except for F (positive control α-fetoprotein) and G (positive control hCG), in which negative control is placed in the upper left corner. C–G: serial sections. Bar corresponds to 20 μm.

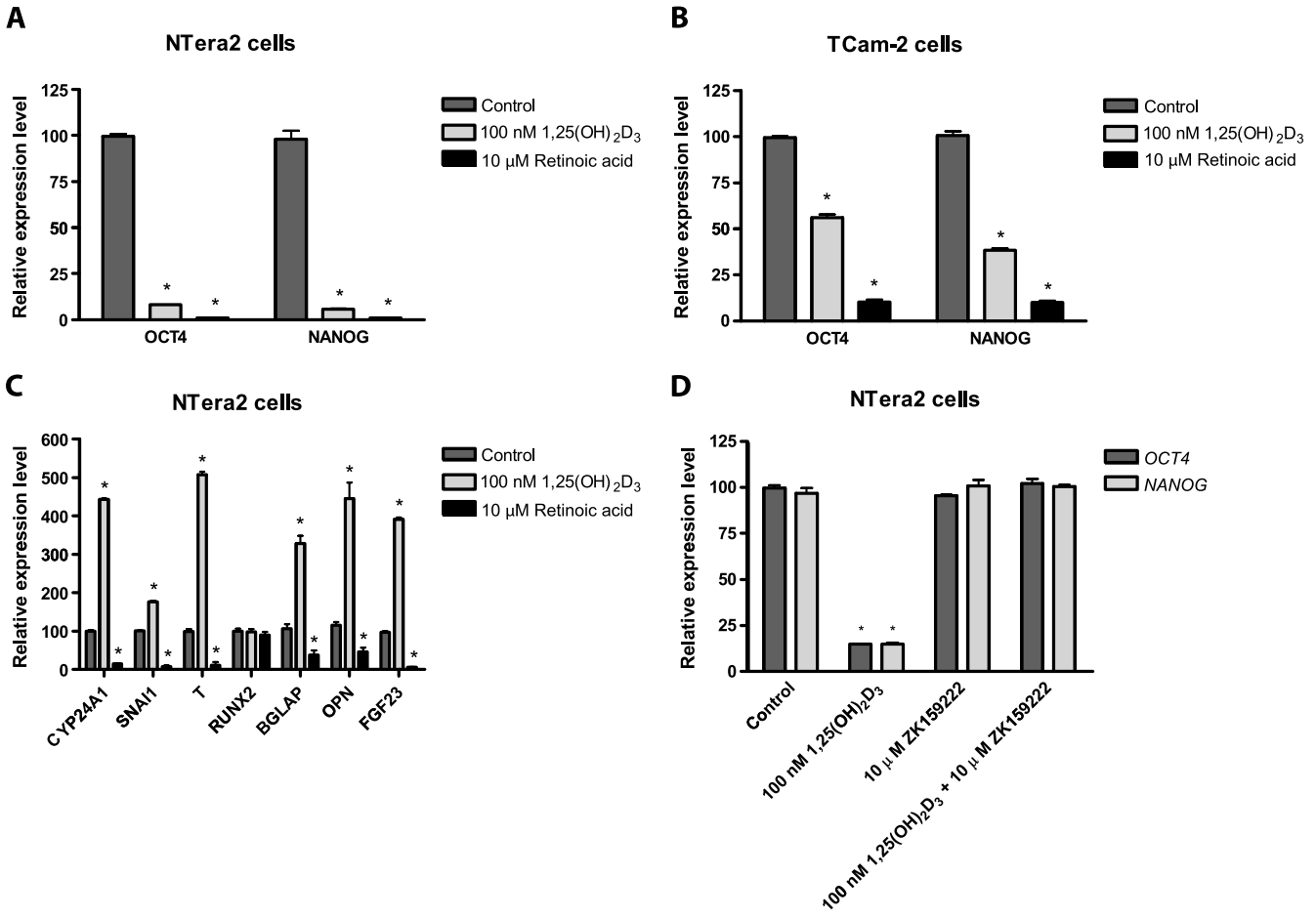

Figure 3. Gene expression following treatment with $1,25(OH)_2D_3$, RA, and DMSO in NTera2 and TCam-2 cells. (A) *OCT4* and *NAONOG* expression in NTera2 cells. (B) OCT4 and *NANOG* expression in TCam-2 cells. (C) Expression of *CYP24A1*, *SNAI1*, *T* (*brachyury*), *RUNX2*, *BGLAP* (*osteocalcin*), *OPN*, and *FGF23* in NTera2 cells. (D) Effect of VDR antagonist ZK159222 on expression of pluripotency genes. All cells are treated with either 100 nM $1,25(OH)_2D_3$, 10 μM RA, or DMSO for 18 days. Except for (D) where cells were treated 6 days. Expression is normalized to β2M and expression level at day 0. Values represent mean ± SD. All experiments are conducted in triplicates and have been repeated twice. Note different scales. *$P < .01$.

two-fold and *NANOG* expression three-fold after 18 days of treatment (both $P < .001$; Figure 3).

Morphologic changes of the cells were observed during $1,25(OH)_2D_3$ treatment of NTera2 cells: condensation and flattening of the nucleus, accumulation of vesicles/droplets in the nucleus and cytoplasm, and lower nuclear/cytoplasmic ratio. However, $1,25(OH)_2D_3$ did not induce the neuron-like transformation of NTera2 cells that was observed after RA treatment (Figure 4). The modest down-regulation of both pluripotency markers in TCam-2 cells was accompanied by only discrete morphologic changes limited to a minor increase in vesicles/droplets following treatment with either RA or $1,25(OH)_2D_3$. Longer treatment periods (up to 30 days) with $1,25(OH)_2D_3$ caused no additional morphologic effects, and the transcriptional level of *OCT4* and *NANOG* remained constant after 2 days in NTera2 cells and 8 days in TCam-2 cells (Figure W4). Down-regulation of *OCT4* and *NANOG* in $1,25(OH)_2D_3$-treated NTera2 cells was coincidental with significant ($P < .001$) up-regulation of mesodermal markers: *brachyury* (*T*) (four-fold) and *SNAI1* (two-fold). Furthermore, $1,25(OH)_2D_3$ upregulated classic bone markers significantly ($P < .001$): *CYP24A1* (four-fold), *FGF23* (three-fold), gla/*BGLAP* (three-fold), and *OPN* (four-fold) (Figure 3). Interestingly, neither mesodermal nor bone markers were upregulated following RA treatment in NTera2 cells. Instead, RA mediated a down-regulation: *SNAI1* (4-fold), *brachyury* (*T*) (28-fold), *CYP24A1* (5-fold), *gla* (3-fold), *OPN* (3-fold), and *FGF23* (63-fold) (all $P < .001$; Figure 3).

The transcriptional changes in both cell lines were supported by ICC analysis (Figure 4). OCT4 was expressed in the nuclei of both TCam-2 and NTera2 cells, and the protein levels matched the transcriptional changes in both cell lines. OCT4 expression diminished rapidly following treatment with RA and $1,25(OH)_2D_3$, but OCT4 was detected in a larger fraction of TCam-2 cells compared with NTera2 cells. VDR was expressed in the nucleus of both cell lines, and VDR expression appeared higher in RA- and vehicle-treated cells compared with $1,25(OH)_2D_3$-treated cells (Figure 4). IHC revealed the highest CYP24A1 expression in NTera2 cells following RA treatment (Figure 4), whereas western blot (WB) supported the transcriptional changes with highest CYP24A1 level in control and $1,25(OH)_2D_3$-treated NTera2 cells (Figure W5). Surprisingly, bone markers such as FGF23 and osteocalcin were expressed in both cell lines before treatment (Figure 4). The cytoplasmic FGF23 expression was high in NTera2 cells and increased following $1,25(OH)_2D_3$

treatment. In contrast, RA lowered FGF23 protein expression substantially, which was in line with the observed transcriptional downregulation (Figures 3*C* and 4). FGF23 was also detected in TCam-2 cells, although with low intensity compared with NTera2 cells. Osteocalcin (gla, BGLAP) was primarily expressed in vesicles/droplets within the nucleus of both cell lines. However, a weak cytoplasmic expression was noticed in ~15% of the cells, which seemed to increase in $1,25(OH)_2D_3$-treated cells. Especially in TCam-2 cells, the cytoplasmic osteocalcin (gla, BGLAP) expression increased, but the changes were modest and not reflecting the large transcriptional changes (Figures 3*C* and 4). Another bone marker, OPN, was not expressed in NTera2 cells at the protein level. However, a weak cytoplasmic expression was found in 10% to 15% of control and $1,25(OH)_2D_3$-treated TCam-2 cells, whereas OPN was undetectable in RA-treated cells (Figure 4). 2102Ep was also treated with RA and $1,25(OH)_2D_3$, but no difference in *OCT4* or *NANOG* expression was found after 18 days of treatment (Figure W5).

To establish whether the observed effects of $1,25(OH)_2D_3$ were mediated through VDR, we treated NTera2 cells for 8 days simultaneously with $1,25(OH)_2D_3$ and the specific genomic VDR antagonist (ZK159222). ZK159222 abrogated the $1,25(OH)_2D_3$-mediated effect on *OCT4* and *NANOG* completely (Figure 3*D*). NTera2 cells were treated with 0.1 to 1 μM $25(OH)D_3$ for 18 days without any effect on *OCT4* and *NANOG* expression or cell morphology (Figure W5). WB confirmed that NTera2 cells had no expression of CYP27B1. The peroxisome proliferator-activated receptor gamma (PPARγ) agonist rosiglitazone was also tested in NTera2 cells but had no effect on the expression of the pluripotency factors (Figure W4).

Influence of $1,25(OH)_2D_3$ on NTera2 Tumor Formation and Growth In Vivo

We subsequently investigated whether the embryonic cell differentiating ability of VD was effective in stunting growth of NTera2 cells forming EC-like tumors *in vivo* in a nude mouse model. Almost all animals (34 of 35) developed tumors in the study period. Neither onset of tumor formation (12–15 days) nor average tumor size differed significantly between left and right flanks (Figure 5). Pretreatment with cholecalciferol-supplemented diet (1100 IU) from the time of inoculation did not influence onset of tumor formation or tumor size compared with vehicle-treated (600 IU) animals (Figure 5). The variation in tumor size within the groups was substantial and increased with tumor burden in the animals not receiving cisplatin, and at day 28, the majority of animals in these groups were sacrificed because of large tumor burden. $1,25(OH)_2D_3$-treated tumors tended to grow slower than those treated with vehicle, whereas cholecalciferol-treated tumors seemed to grow faster, but the differences were not significant ($P > .05$; Figure 5). Cisplatin-treated animals had a significantly ($P < .05$) lower tumor growth and reduced total tumor size compared with vehicle (Figure 5). Tumor volume was only borderline significant ($P = .07$) when comparing tumors on each flank between cisplatin and non-cisplatin–treated animals at day 28 but significantly ($P = .02$) different when using two-tailed *t* test instead of Bonferroni. A minor randomization

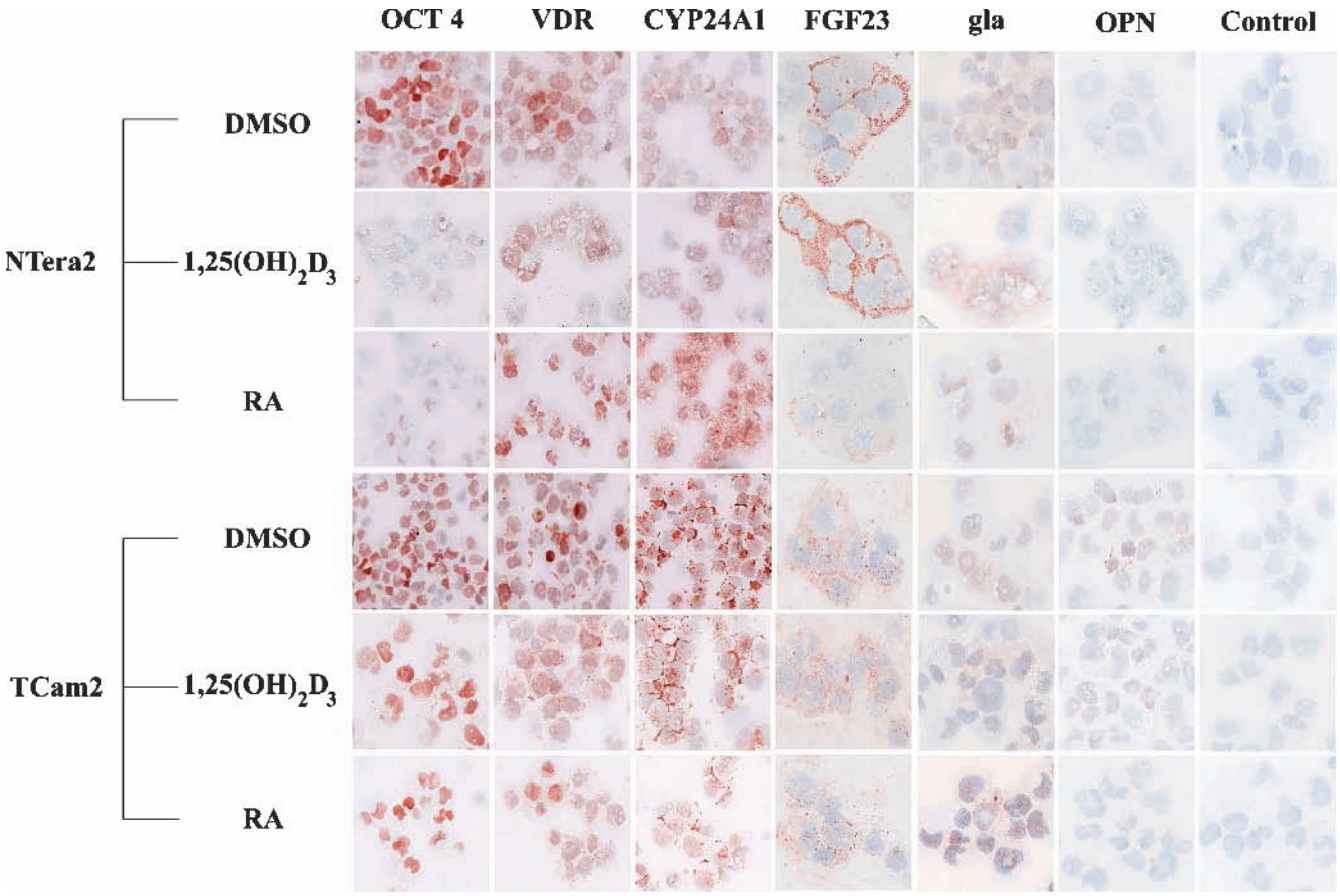

Figure 4. ICC expression of OCT4, VDR, CYP24A1, FGF23, gla (osteocalcin), OPN, and negative control in NTera2 and TCam-2 cells treated with DMSO, 100 nM $1,25(OH)_2D_3$, or 10 μM RA for 18 days.

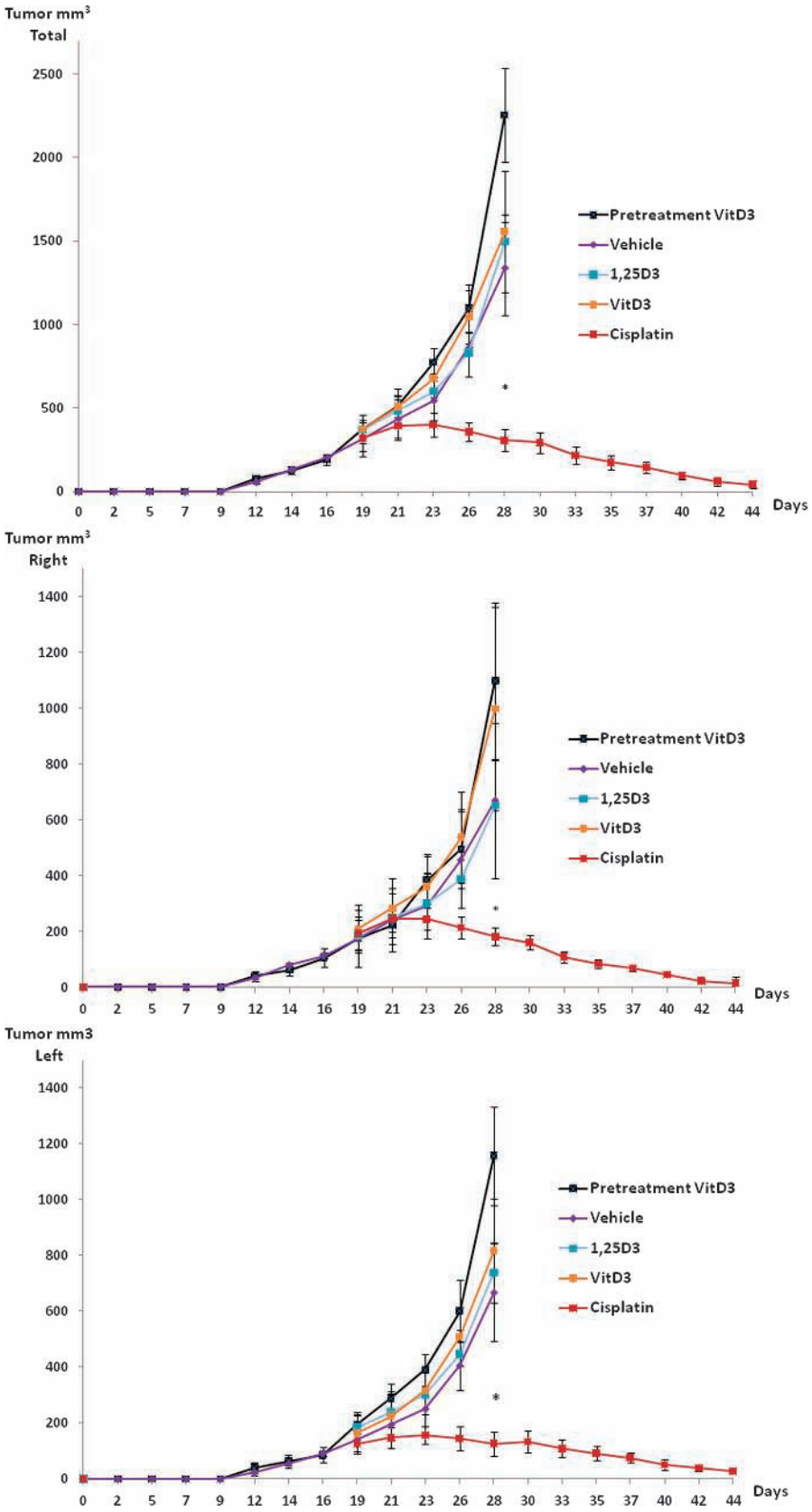

Figure 5. Influence of VD on NTera2 xenograft tumors. Graphs show total tumor burden for each mice tumor growth on the right [pretreated with 100 nM $1,25(OH)_2D_3$ for 20 days] and left flanks (vehicle) until day 19. Seven mice received cholecalciferol-supplemented diet (1100 IU/kg) from the day of inoculation, whereas 28 mice received standard chow (600 IU/kg). At day 19, the 28 animals were randomized to four different treatment groups: 1) control received vehicle (0.1% ethanol in sterile saline) three times weekly i.p., 2) cisplatin (6 mg/kg) i.v. once weekly, 3) calcitriol (0.05 μg) i.p. three times weekly, and 4) fortified diet with cholecalciferol (1100 IU D_3/kg diet). Values represent mean ± SEM. *$P < .05$.

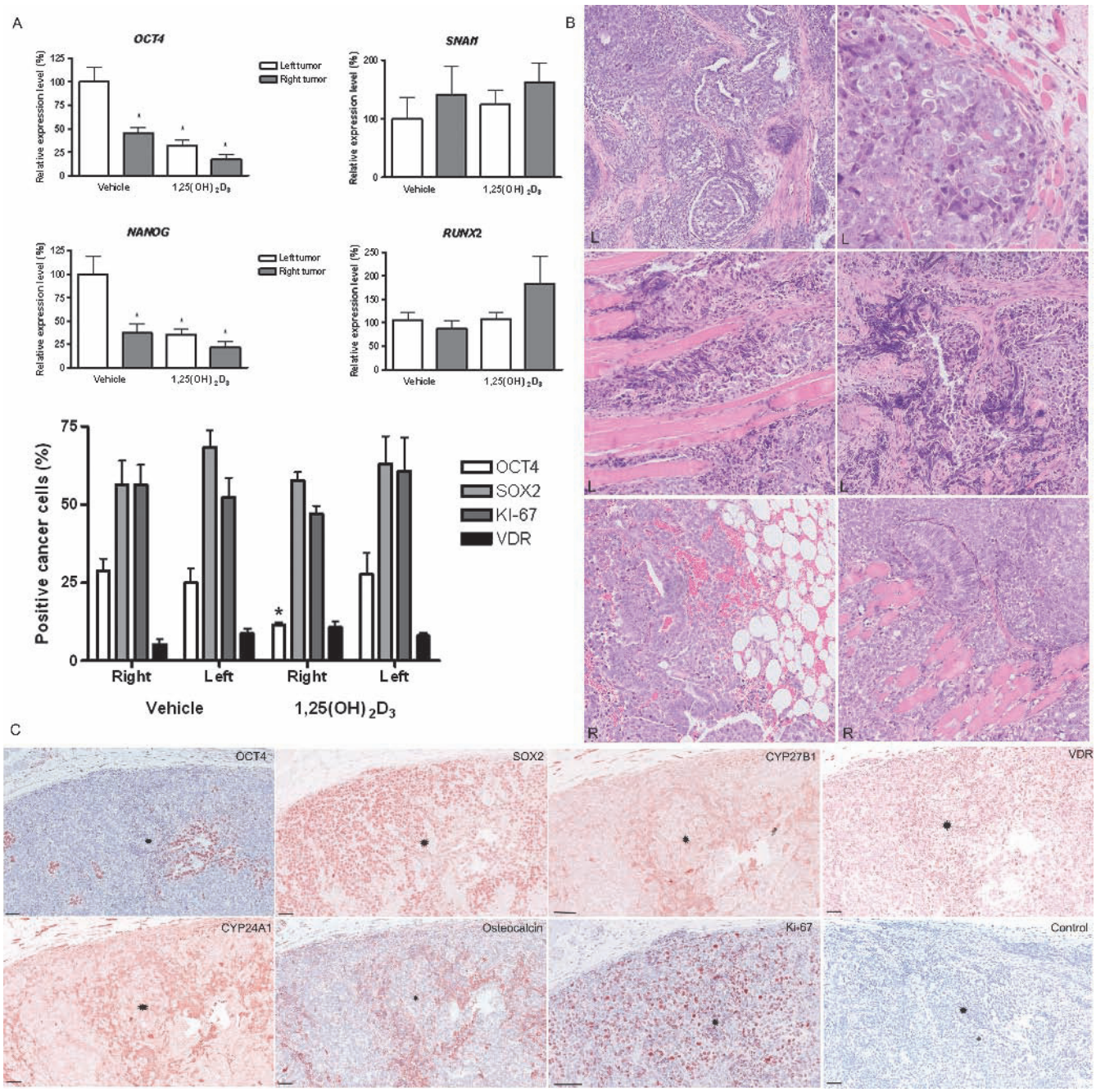

Figure 6. Changes in histology, gene, and protein expression following treatment with $1,25(OH)_2D_3$ in NTera2 xenograft tumors. (A) Changes in gene expression of *OCT4*, *NANOG*, *CYP24A1*, *SNAI1*, and *Runx2*. Expression is normalized to β2M and expression level at day 0. All experiments are conducted in triplicates and have been repeated twice. Note different scales. *$P < .05$. Changes in cellular protein expression (OCT4, SOX2, KI-67, and VDR) evaluated by IHC in the right- and left-sided tumors from animals treated *in vivo* with vehicle or $1,25(OH)_2D_3$. Data presented as mean ± SEM. (B) Hematoxylin and eosin stainings of xenograft tumors from right and left flanks. NTera2 cells invaded the surrounding muscle and adipose tissue. Notice the aberrant morphology in a subpopulation of the left-sided NTera2 xenograft cells. R: right-sided tumor. L: left-sided tumor. (C) IHC on serial sections of OCT4, SOX2, CYP27B1, VDR, CYP24A1, osteocalcin (gla), and Ki-67 in representative NTera2 xenograft tumors.

failure resulted in the lowest tumor burden for vehicle- and cisplatin-treated animals initially. Therefore, differences between groups were also calculated (not significant) by using an index value (normalized to control) and a proportional increase in tumor size (normalized to tumor size at randomization). After adjustment, the proportional tumor increase was borderline significantly ($P = .08$) lower on the right compared with the left flank of $1,25(OH)_2D_3$-treated mice (Figure 5).

Histologic Phenotype and Gene Expression in NTera2 Xenografts

Finally, we investigated the xenograft tumors for possible VD-induced cell differentiation. The xenograft tumors invaded the surrounding adipose tissue and skeletal muscle independently of treatment regime. The histologic appearance varied depending on the distance of the human tumor cells to the niche of surrounding mouse

somatic tissue. On the left flank, the tumors were more heterogeneous, comprising mainly EC-resembling NTera2 cells, but also more differentiated glandular structures and embryoid bodies were found (Figure 6*B*). In the vicinity of the somatic tissue, a larger proportion of the tumor cells presented with thin elongated cytoplasm and nuclei (Figure 6*B*). Only 25% of the tumor cells expressed OCT4 in the nucleus, whereas a larger fraction (62%) expressed SOX2 (Figure 6*A*). The fraction of OCT4-positive cells differed significantly ($P < .05$) between tumors from vehicle- and $1,25(OH)_2D_3$-treated animals (Figure 6). The IHC difference was matched by the significant ($P < .05$) transcriptional differences in tumors receiving treatment with $1,25(OH)_2D_3$ either pretumor or posttumor formation (Figure 6). Besides *OCT4*, also *NANOG* was downregulated by $1,25(OH)_2D_3$ ($P < .05$) compared with vehicle, whereas *RUNX2* and *SNAI1* levels tended to be higher ($P > .05$). The high growth rate was reflected by several mitotic cells, and accordingly, 54% of the xenograft tumor cells expressed Ki-67 in the nucleus. Surprisingly, VDR expression was much lower in the tumor-forming NTera2 cells compared with NTera2 cells before inoculation. Most tumor cells without VDR expression were also OCT4-negative. The few VDR-positive tumor cells in the xenograft tumors appeared thin and elongated. They coexpressed CYP27B1, CYP24A1, osteocalcin (gla, BGLAP), and SOX2 (Figure 6*C*), and some of these cells were also mitotic (Ki-67–positive).

Discussion

This study established that active VD is capable of differentiating EC cells by down-regulation of pluripotency genes and inducing a mesenchymal transition toward an osteogenic phenotype in TGCT-derived cell lines *in vitro* and in an *in vivo* model of NTera2 xenografts. These findings are in accordance with our observations in human tissue samples where expression of VDR and VD-metabolizing enzymes markedly diminished in invasive TGCTs in comparison to preinvasive CIS.

In agreement with the presumed fetal origin of CIS, we found VDR expression in fetal gonocytes and prespermatogonia, which may imply a role for VD in early development of germ cells. Noteworthy, VDR was mainly detected in the cytoplasm of CIS cells, whereas the receptor was expressed in both nucleus and cytoplasm of normal gonocytes. The subcellular location of VDR indicates whether it mediates genomic effects in the nucleus or fast nongenomic effects in the cytoplasm [16]. However, the location of VDR is also influenced by substrate availability, which is largely determined by the expression level of the inactivating enzyme CYP24A1 [17,18]. Abundant expression of CYP24A1 in CIS cells may thus reduce substrate availability, which subsequently results in decreased transcription of VDR and VD-regulated genes [16–20]. VDR has previously been detected in TGCT [21], but the presence of VDR in human fetal germ cells has, to our knowledge, not been shown before and supports a role for VD during germ cell development, which requires further studies to establish precise mechanisms.

The molecular events leading to progression of CIS to seminomas involve increased proliferation and survival, whereas the events leading to nonseminomas remain unknown, except that a substantial reprogramming is associated with a gain of the short arm of chromosome 12 [6,22,23]. Noteworthy, 12p contains, besides NANOG and other pluripotency factors, genes encoding parathyroid hormone-related peptide (PTHrP) and FGF23, which, in addition to Klotho, calcitonin, calcium, and $1,25(OH)_2D_3$, are main regulators of systemic VD metabolism [17,24–28]. We show here for the first time that FGF23 is expressed in NTera2 and TCam-2 cells, indicating that FGF23 may be a regulatory factor in TGCT and influence the Klotho-expressing tissue in the vicinity of the tumors [29,30]. The undifferentiated component of nonseminomas, EC cells, resemble hESC and possess the ability to differentiate into multiple somatic lineages [31]. We established in this study that, in contrast to CIS, EC cells had none or low expression of VDR and VD-metabolizing enzymes, suggesting that this pathway was downregulated during the progression from CIS to EC. By contrast, cellular VD metabolism was partially retained in the less aggressive seminomas, consistent with their CIS-like phenotype [6,32]. Our data are in agreement with previous observations in cancers of colon, prostate, kidney, and mammary gland, where the expression of CYP27B1 and VDR is downregulated during malignant transformation into invasive metastatic tumors. The diminished expression reduces the cellular responsiveness to the circulating forms of VD and may affect both invasiveness and tumor growth [33].

Interestingly, VD metabolism appears to be reestablished during tumor differentiation as it was also present in differentiated somatic and extraembryonic components of teratomas. In an apparently transitional population of EC cells that lost OCT4 but retained SOX2 expression, we found nuclear VDR expression concomitant with cytoplasmic expression of the VD-metabolizing enzymes. The observed nuclear coexpression with SOX2 indicates that VDR through its genomic pathway might be involved in differentiation into a somatic phenotype [34]. This is supported by the cytoplasmic expression of the VD-regulated gene *BGLAP* (osteocalcin) in these cells [35]. The cytoplasmic osteocalcin expression found in both TGCTs and NTera2 tumor xenografts indicates that the VDR-positive tumor cells possess bone characteristics, because osteocalcin is incompletely spliced in nonosseous tissues [36].

VD-induced embryonic differentiation toward bone tissue has been only demonstrated in a murine model. Mouse embryonic stem cells expressed early osteoblast markers, such as Runx2 and alkaline phosphatase, as well as late markers, such as OPN and osteocalcin, following combination treatment with $1,25(OH)_2D_3$, ascorbic acid, and β-glycerophosphate [37–39]. Our *in vitro* studies showed that $1,25(OH)_2D_3$ alone induced differentiation of both seminoma-derived TCam-2 cells and EC-like NTera2 cells. To our knowledge, this is the first time $1,25(OH)_2D_3$ has been shown to induce differentiation of pluripotent cancer stem cells, manifested by down-regulation of essential pluripotency factors OCT4 and NANOG, coincident with up-regulation of mesodermal markers SNAI1, T (brachyury), and bone markers OPN, osteocalcin, and FGF23 in NTera2 cells. The observed dose-response relationship between all $1,25(OH)_2D_3$ concentrations $\geq$1 nM and the transcriptional changes indicates a receptor-mediated response [40]. This was further supported by the specific genomic VDR antagonist ZK159222 that abrogated the $1,25(OH)_2D_3$-mediated down-regulation of *OCT4* and *NANOG* completely. SNAI1, known to promote mesodermal commitment by repressing ectodermic markers [41], was upregulated and may drive the $1,25(OH)_2D_3$-mediated mesenchymal transition toward an osteogenic phenotype in the EC cells [29].

Some of the $1,25(OH)_2D_3$-induced transcriptional changes were not matched at the protein level. Especially, the marked up-regulation of *OPN* and *BGLAP* in NTera2 cells was not found after IHC and only minor morphologic changes were observed in the cells [36]. This may be due to incomplete differentiation and retained germ cell characteristics of NTera2. This was supported by the lack of *RUNX2*

induction by $1,25(OH)_2D_3$, which may cause translational repression of osteogenic markers, for instance, OPN that is known to be expressed in other solid cancers and involved in invasiveness [42]. Noteworthy, osteocalcin was virtually not expressed at the protein level after $1,25(OH)_2D_3$ treatment *in vitro*, but it was expressed in the NTera2 xenograft tumors indicating that other factors besides VD present *in vivo* are mandatory to complete osteogenic differentiation of NTera2 cells. Surprisingly, FGF23 was expressed in NTera2 and TCam-2 cells before treatment and markedly upregulated following $1,25(OH)_2D_3$ treatment of NTera2 cells. In agreement with the effect on mesenchymal stem cells, $1,25(OH)_2D_3$ mediated differentiation of NTera2 cells toward an osteogenic phenotype. The treatment clearly differed from the RA-induced differentiation toward a neuroectodermal phenotype [43], which is associated with down-regulation of the mesodermal and osteogenic markers, including FGF23 [29,45].

In the *in vivo* model, $1,25(OH)_2D_3$-pretreated NTera2 cells formed xenograft tumors simultaneously with the vehicle-treated cells inoculated on the other flank. Furthermore, tumor growth was similar on both sides and the histologic appearance was not markedly different, although cellular morphology appeared less heterogeneous in $1,25(OH)_2D_3$-pretreated tumors. We speculate that it may be due to the partial differentiation induced by $1,25(OH)_2D_3$, which may result in the presence of less cancer cells with sustained OCT4 and NANOG expression, although evidently enough to produce an aggressive tumor when a substantial number of cancer cells are inoculated. Contrary to our expectations, cholecalciferol supplements given either pretumor or posttumor formation as well as treatment with $1,25(OH)_2D_3$ after tumor formation did not diminish tumor formation or growth. The insignificant antitumor effects observed in this study may be improved by using higher doses of $1,25(OH)_2D_3$, although the selected dose of 0.05 μg (three times a week) has proven to be efficient in other xenograft tumors [46]. In addition, cholecalciferol treatments did not significantly affect tumor growth. This may be due to the low difference in cholecalciferol dose (1100 IU *versus* 600 IU) between treated and control animals, respectively, which may be inadequate to detect a significant difference in tumor growth. We selected the cholecalciferol doses based on a previous kinetics study conducted in rodents, where doses from 500 to 1000 IU gave a marked increase in endogenous $1,25(OH)_2D_3$ [47]. A recent study showed antitumor effects with a much higher dose of 5000 IU cholecalciferol [45], which imply that the dose used in our study may be too low. We used a high cisplatin dose that proved very efficient in treating the xenograft tumors, which imply that the model is suitable to test factors for putative antitumor activity. The clinical relevance of VD treatment of TGCTs cannot be fully evaluated by our study design. However, despite the insignificant tumor reduction following $1,25(OH)_2D_3$ treatment, we still found a significant down-regulation of pluripotency factors *in vivo* on both transcriptional and protein levels.

In conclusion, VD metabolism is present in germ cells throughout development and is retained in neoplastic CIS cells, but this pathway is partly silenced during the malignant transition to invasive TGCTs. Active VD, $1,25(OH)_2D_3$, is capable of inducing a partial differentiation of EC cells by down-regulating pluripotency genes and promoting a mesenchymal transition toward an osteogenic phenotype *in vitro* and *in vivo*. However, the differentiation-inducing effects of $1,25(OH)_2D_3$ treatment caused no significant inhibition of tumor growth in NTera2 xenograft tumors in nude mice. Taken together, these findings identify VD as a differentiation factor of cells with embryonic stem cell characteristics, point to a role for VD metabolism during fetal development, and indicate a possible role in the pathogenesis of TGCTs.

Acknowledgments

We thank Dr Peter W. Andrews for a kind gift of NTera2 and 2102Ep cells, Drs Sohei Kitazawa and Janet Shipley for TCam-2 cells, and Giulio Spagnoli for the MAGE-A4 antibody. We gratefully acknowledge several urologists and pathologists of the Greater Copenhagen area hospitals for their help with collecting the tissue samples, especially Dr Niels Græm for fetal specimens. We thank Betina F. Nielsen, Ana R. Nielsen, and Brian V. Hansen for skillful technical assistance, and Neil Harrison, David M. Kristensen, Niels Jørgensen, and Niels Erik Skakkebaek for advice and fruitful discussions. We appreciate the efforts by Carsten L. Buus and Klaus Kristensen from Pipeline Biotech, who performed the xenografting.

References

[1] Sonne SB, Almstrup K, Dalgaard M, Juncker AS, Edsgard D, Ruban L, Harrison NJ, Schwager C, Abdollahi A, Huber PE, et al. (2009). Analysis of gene expression profiles of microdissected cell populations indicates that testicular carcinoma *in situ* is an arrested gonocyte. *Cancer Res* **69**, 5241–5250.

[2] Kristensen DM, Sonne SB, Ottesen AM, Perrett RM, Nielsen JE, Almstrup K, Skakkebaek NE, Leffers H, and Rajpert-De Meyts E (2008). Origin of pluripotent germ cell tumours: the role of microenvironment during embryonic development. *Mol Cell Endocrinol* **288**, 111–118.

[3] Skakkebaek NE, Berthelsen JG, and Muller J (1982). Carcinoma-in-situ of the undescended testis. *Urol Clin North Am* **9**, 377–385.

[4] Ulbright TM (1993). Germ cell neoplasms of the testis. *Am J Surg Pathol* **17**, 1075–1091.

[5] Chaganti RS and Houldsworth J (2000). Genetics and biology of adult human male germ cell tumors. *Cancer Res* **60**, 1475–1482.

[6] Looijenga LH, Gillis AJ, Stoop H, Biermann K, and Oosterhuis JW (2011). Dissecting the molecular pathways of (testicular) germ cell tumour pathogenesis; from initiation to treatment-resistance. *Int J Androl* **34**, e234–e251.

[7] Skotheim RI, Lind GE, Monni O, Nesland JM, Abeler VM, Fossa SD, Duale N, Brunborg G, Kallioniemi O, Andrews PW, et al. (2005). Differentiation of human embryonal carcinomas *in vitro* and *in vivo* reveals expression profiles relevant to normal development. *Cancer Res* **65**, 5588–5598.

[8] Looijenga LH, Gillis AJ, Stoop HJ, Hersmus R, and Oosterhuis JW (2007). Chromosomes and expression in human testicular germ-cell tumors: insight into their cell of origin and pathogenesis. *Ann N Y Acad Sci* **1120**, 187–214.

[9] Gocek E and Studzinski GP (2009). Vitamin D and differentiation in cancer. *Crit Rev Clin Lab Sci* **46**, 190–209.

[10] Bouillon R, Eelen G, Verlinden L, Mathieu C, Carmeliet G, and Verstuyf A (2006). Vitamin D and cancer. *J Steroid Biochem Mol Biol* **102**, 156–162.

[11] Blomberg Jensen M (2012). Vitamin D metabolism, sex hormones, and male reproductive function. *Reproduction* **144**, 135–152.

[12] Blomberg Jensen M and Dissing S (2012). Non-genomic effects of vitamin D in human spermatozoa. *Steroids* **77**, 903–909.

[13] Krishnan AV and Feldman D (2011). Mechanisms of the anti-cancer and anti-inflammatory actions of vitamin D. *Annu Rev Pharmacol Toxicol* **51**, 311–336.

[14] Blomberg Jensen M, Andersen CB, Nielsen JE, Bagi P, Jorgensen A, Juul A, and Leffers H (2010). Expression of the vitamin D receptor, 25-hydroxylases, 1α-hydroxylase and 24-hydroxylase in the human kidney and renal clear cell cancer. *J Steroid Biochem Mol Biol* **121**, 376–382.

[15] Blomberg Jensen M, Nielsen JE, Jorgensen A, Rajpert-De Meyts E, Kristensen DM, Jorgensen N, Skakkebaek NE, Juul A, and Leffers H (2010). Vitamin D receptor and vitamin D metabolizing enzymes are expressed in the human male reproductive tract. *Hum Reprod* **25**, 1303–1311.

[16] Deeb KK, Trump DL, and Johnson CS (2007). Vitamin D signalling pathways in cancer: potential for anticancer therapeutics. *Nat Rev Cancer* **7**, 684–700.

[17] Healy KD, Frahm MA, and DeLuca HF (2005). 1,25-Dihydroxyvitamin D_3 up-regulates the renal vitamin D receptor through indirect gene activation and receptor stabilization. *Arch Biochem Biophys* **433**, 466–473.

[18] Ebert R, Schutze N, Adamski J, and Jakob F (2006). Vitamin D signaling is modulated on multiple levels in health and disease. *Mol Cell Endocrinol* **248**, 149–159.

[19] Chung I, Karpf AR, Muindi JR, Conroy JM, Nowak NJ, Johnson CS, and Trump DL (2007). Epigenetic silencing of CYP24 in tumor-derived endothelial cells contributes to selective growth inhibition by calcitriol. *J Biol Chem* **282**, 8704–8714.

[20] Haussler MR, Jurutka PW, Mizwicki M, and Norman AW (2011). Vitamin D receptor (VDR)-mediated actions of $1\alpha,25(OH)_2$vitamin D_3: genomic and non-genomic mechanisms. *Best Pract Res Clin Endocrinol Metab* **25**, 543–559.

[21] Nangia AK, Hill O, Waterman MD, Schwender CE, and Memoli V (2007). Testicular maturation arrest to testis cancer: spectrum of expression of the vitamin D receptor and vitamin D treatment *in vitro*. *J Urol* **178**, 1092–1096.

[22] Korkola JE, Houldsworth J, Chadalavada RS, Olshen AB, Dobrzynski D, Reuter VE, Bosl GJ, and Chaganti RS (2006). Down-regulation of stem cell genes, including those in a 200-kb gene cluster at 12p13.31, is associated with *in vivo* differentiation of human male germ cell tumors. *Cancer Res* **66**, 820–827.

[23] Oosterhuis JW and Looijenga LH (2005). Testicular germ-cell tumours in a broader perspective. *Nat Rev Cancer* **5**, 210–222.

[24] Yang W, Friedman PA, Kumar R, Omdahl JL, May BK, Siu-Caldera ML, Reddy GS, and Christakos S (1999). Expression of $25(OH)D_3$ 24-hydroxylase in distal nephron: coordinate regulation by $1,25(OH)_2D_3$ and cAMP or PTH. *Am J Physiol* **276**, E793–E805.

[25] Shimada T, Hasegawa H, Yamazaki Y, Muto T, Hino R, Takeuchi Y, Fujita T, Nakahara K, Fukumoto S, and Yamashita T (2004). FGF-23 is a potent regulator of vitamin D metabolism and phosphate homeostasis. *J Bone Miner Res* **19**, 429–435.

[26] Shinki T, Ueno Y, DeLuca HF, and Suda T (1999). Calcitonin is a major regulator for the expression of renal 25-hydroxyvitamin D_3-1α-hydroxylase gene in normocalcemic rats. *Proc Natl Acad Sci USA* **96**, 8253–8258.

[27] Healy KD, Vanhooke JL, Prahl JM, and DeLuca HF (2005). Parathyroid hormone decreases renal vitamin D receptor expression *in vivo*. *Proc Natl Acad Sci USA* **102**, 4724–4728.

[28] Lanske B and Razzaque MS (2007). Vitamin D and aging: old concepts and new insights. *J Nutr Biochem* **18**, 771–777.

[29] de Frutos CA, Dacquin R, Vega S, Jurdic P, Huca-Gayet I, and Nieto MA (2009). Snail1 controls bone mass by regulating Runx2 and VDR expression during osteoblast differentiation. *EMBO J* **28**, 686–696.

[30] Kommagani R, Caserta TM, and Kadakia MP (2006). Identification of vitamin D receptor as a target of p63. *Oncogene* **25**, 3745–3751.

[31] Clark AT (2007). The stem cell identity of testicular cancer. *Stem Cell Rev* **3**, 49–59.

[32] Rajpert-De Meyts E and Hoei-Hansen CE (2007). From gonocytes to testicular cancer: the role of impaired gonadal development. *Ann N Y Acad Sci* **1120**, 168–180.

[33] Fleet JC (2008). Molecular actions of vitamin D contributing to cancer prevention. *Mol Aspects Med* **29**, 388–396.

[34] Sonne SB, Perrett RM, Nielsen JE, Baxter MA, Kristensen DM, Leffers H, Hanley NA, and Rajpert-De-Meyts E (2010). Analysis of SOX2 expression in developing human testis and germ cell neoplasia. *Int J Dev Biol* **54**, 755–760.

[35] Haussler MR, Haussler CA, Bartik L, Whitfield GK, Hsieh JC, Slater S, and Jurutka PW (2008). Vitamin D receptor: molecular signaling and actions of nutritional ligands in disease prevention. *Nutr Rev* **66**, 98–112.

[36] Jung C, Ou YC, Yeung F, Frierson HF Jr, and Kao C (2001). Osteocalcin is incompletely spliced in non-osseous tissues. *Gene* **271**, 143–150.

[37] zur Nieden NI, Kempka G, and Ahr HJ (2003). *In vitro* differentiation of embryonic stem cells into mineralized osteoblasts. *Differentiation* **71**, 18–27.

[38] Akiyama H, Kim JE, Nakashima K, Balmes G, Iwai N, Deng JM, Zhang Z, Martin JF, Behringer RR, Nakamura T, et al. (2005). Osteo-chondroprogenitor cells are derived from Sox9 expressing precursors. *Proc Natl Acad Sci USA* **102**, 14665–14670.

[39] zur Nieden NI, Price FD, Davis LA, Everitt RE, and Rancourt DE (2007). Gene profiling on mixed embryonic stem cell populations reveals a biphasic role for β-catenin in osteogenic differentiation. *Mol Endocrinol* **21**, 674–685.

[40] Rochel N, Wurtz JM, Mitschler A, Klaholz B, and Moras D (2000). The crystal structure of the nuclear receptor for vitamin D bound to its natural ligand. *Mol Cell* **5**, 173–179.

[41] Gill JG, Langer EM, Lindsley RC, Cai M, Murphy TL, Kyba M, and Murphy KM (2011). Snail and the microRNA-200 family act in opposition to regulate epithelial-to-mesenchymal transition and germ layer fate restriction in differentiating ESCs. *Stem Cells* **29**, 764–776.

[42] He B, Mirza M, and Weber GF (2006). An osteopontin splice variant induces anchorage independence in human breast cancer cells. *Oncogene* **25**, 2192–2202.

[43] Andrews PW, Gonczol E, Plotkin SA, Dignazio M, and Oosterhuis JW (1986). Differentiation of TERA-2 human embryonal carcinoma cells into neurons and HCMV permissive cells. Induction by agents other than retinoic acid. *Differentiation* **31**, 119–126.

[44] Mizuno Y, Gotoh A, Kamidono S, and Kitazawa S (1993). Establishment and characterization of a new human testicular germ cell tumor cell line (TCam-2). *Nippon Hinyokika Gakkai Zasshi* **84**, 1211–1218.

[45] Masuyama R, Stockmans I, Torrekens S, Van Looveren R, Maes C, Carmeliet P, Bouillon R, and Carmeliet G (2006). Vitamin D receptor in chondrocytes promotes osteoclastogenesis and regulates FGF23 production in osteoblasts. *J Clin Invest* **116**, 3150–3159.

[46] Swami S, Krishnan AV, Wang JY, Jensen K, Horst R, Albertelli MA, and Feldman D (2012). Dietary vitamin D_3 and 1,25-dihydroxyvitamin D_3 (calcitriol) exhibit equivalent anticancer activity in mouse xenograft models of breast and prostate cancer. *Endocrinology* **153**, 2576–2587.

[47] Fleet JC, Gliniak C, Zhang Z, Xue Y, Smith KB, McCreedy R, and Adedokun SA (2008). Serum metabolite profiles and target tissue gene expression define the effect of cholecalciferol intake on calcium metabolism in rats and mice. *J Nutr* **138**, 1114–1120.

Table W1. Primers Used for RT-PCR and Quantitative PCR.

Gene	Forward Primer	Reverse Primer
CYP2R1	AGAGACCCAGAAGTGTTCCAT	GTCTTTCAGCACAGATGAGGTA
CYP27A1	GGCAAGTACCCAGTACGG	AGCAAATAGCTTCCAAGG
CYP27B1	CCTGGCAGAGCTTGAATTGCA	GGGGAAGATGTATACCTTGGT
VDR	GGAGAAAACACTTGTAAGTTGCT	TGGTCAGGTTGGTCTCGAACT
CYP24A1	GGCCTCTTTCATCACAGAGCT	GCCTATCGCGACTACCGCAA
RPS20	AGACTTTGAGAATCACTACAAGA	ATCTGCAATGGTGACTTCCAC
OCT4 (POU5F1)	GACTCCTCGGTCCCTTTCC	CAAAAACCCTGGCACAAACT
NANOG	TGATTTGTGGGCCTGAAGAAAA	GAGGCATCTCAGCAGAAGACA
SNAI1	CACTATGCCGCGCTCTTTC	GGTCGTAGGGCTGCTGGAA
Brachyury (T)	TCAGCAAAGTCAAGCTCACCA	CCCCAACTCTCACTATGTGGATT
gla (BGLAP)	CACTCCTCGCCCTATTGGC	GCCTGGGTCTCTTCACTACCT
OPN (SPP1)	ACCACATGGATGATATGGATGA	GTCAGGTCTGCGAAACTTCTTA
FGF23	CACCTGCAGATCCACAAGAA	TAATCACCACAAAGCCAGCA
β2M	ATCCAATCCAAATGCGGCATC	AGTATGCCTGCCGTGTGAAC

All primers shown in 5′ to 3′ direction.

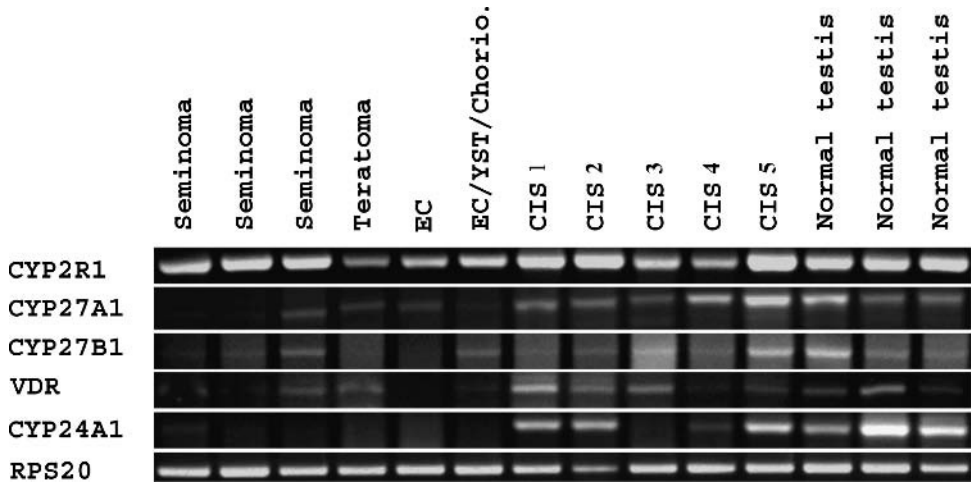

Figure W1. RT-PCR analysis of mRNA expression in malignant and normal samples (EC, embryonal carcinoma; YST, yolk sac tumor; Chorio., choriocarcinoma; CIS, carcinoma *in situ*; CIS1, 70% CIS from EC; CIS2, 70% CIS from seminoma; CIS3, 70% CIS from mixed TGCT; CIS4, 95% CIS; CIS5, 95% CIS).

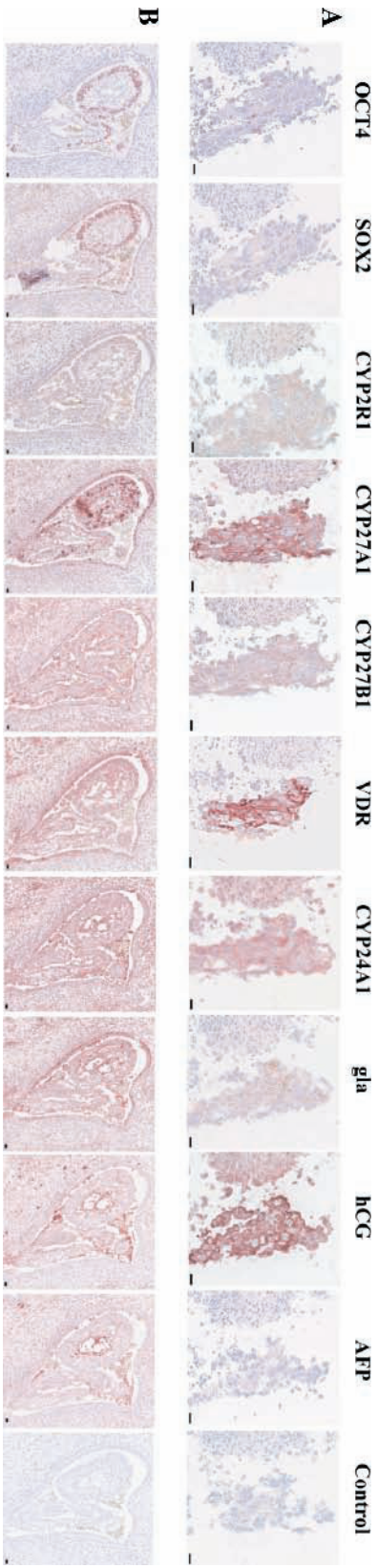

Figure W2. IHC expression in nonseminomas. (A) IHC expression in choriocarcinoma of OCT4, SOX2, CYP2R1, CYP27A1, CYP27B1, VDR, CYP24A1, gla, hCG, AFP, and negative control. (B) IHC expression in mixed nonseminoma of OCT4, SOX2, CYP2R1, CYP27A1, CYP27B1, VDR, CYP24A1, gla (osteocalcin), hCG, AFP, and negative control. All IHC studies were conducted on serial sections. Bar corresponds to 20 μm.

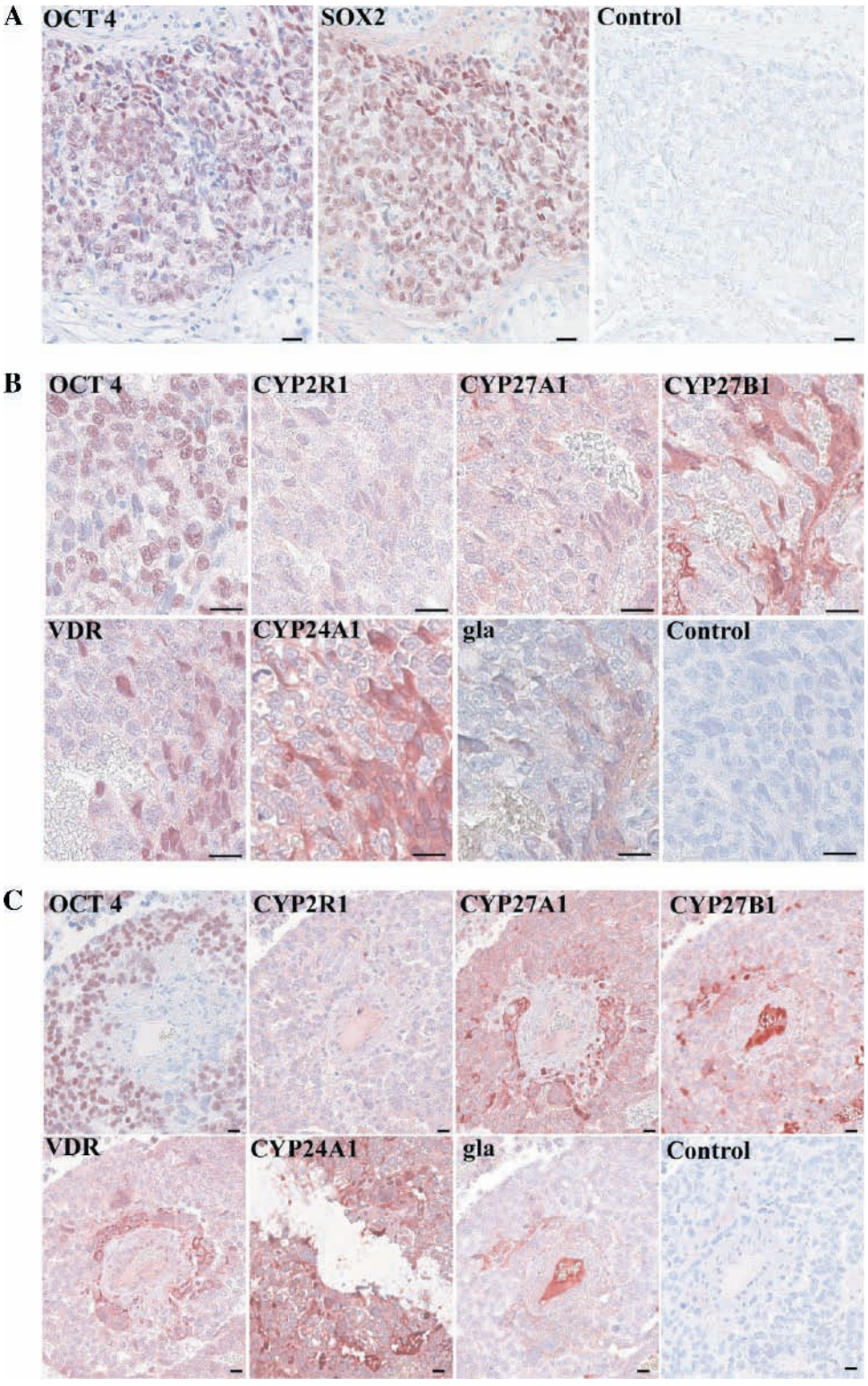

Figure W3. IHC expression in nonseminomas. (A) IHC expression in serial sections from EC of OCT4, SOX2, and negative control. (B) IHC expression in serial sections from EC of OCT4, CYP2R1, CYP27A1, CYP27B1, VDR, CYP24A1, gla (osteocalcin), and negative control. (C) IHC expression in serial sections from mixed nonseminoma of OCT4, CYP2R1, CYP27A1, CYP27B1, VDR, CYP24A1, gla, and negative control. Bar corresponds to 20 μm.

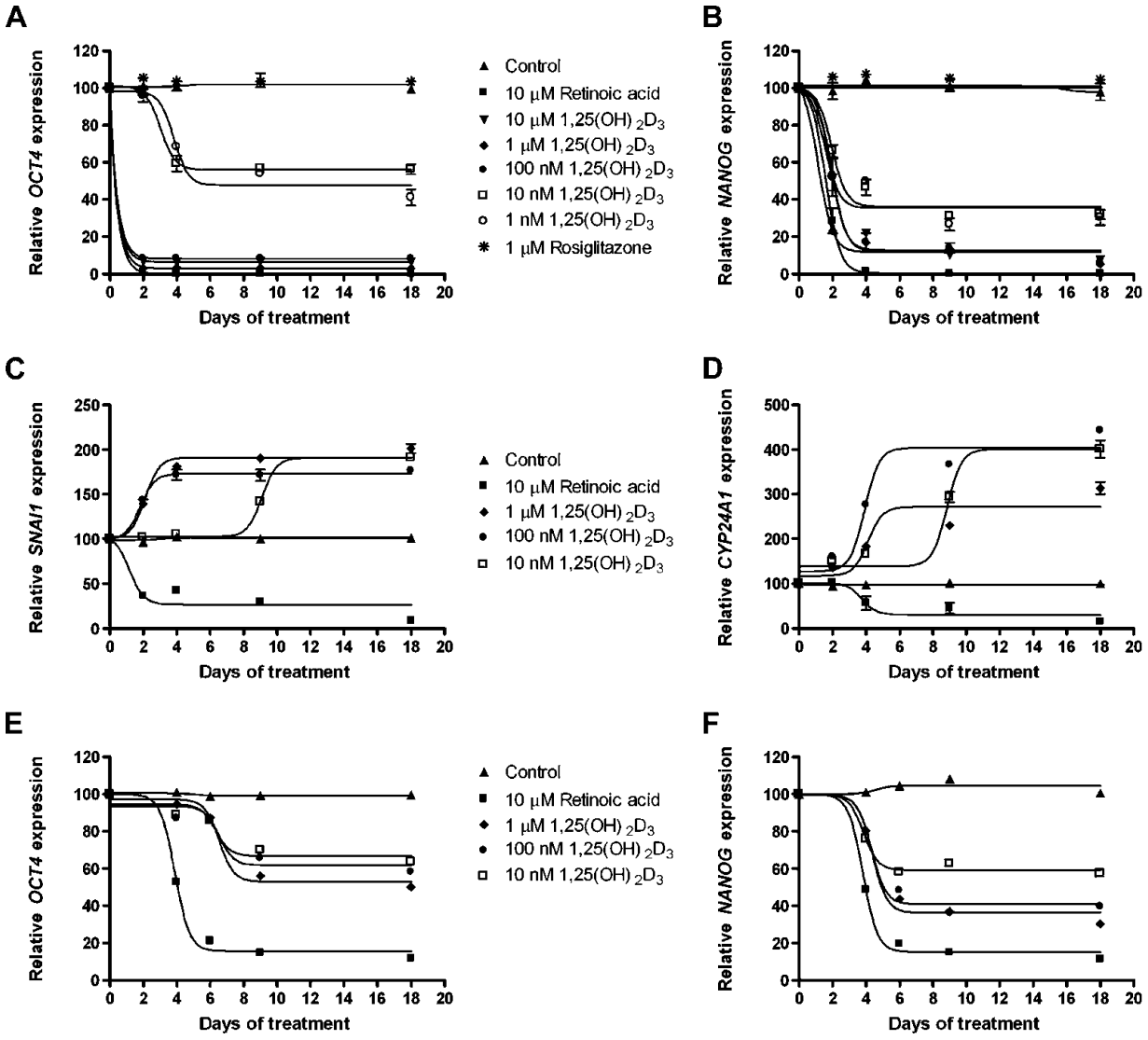

Figure W4. Gene expression following treatment with $1,25(OH)_2D_3$, RA, and DMSO in NTera2 and TCam-2 cells. (A) *OCT4* expression in NTera2 cells. (B) *NANOG* expression in NTera2 cells. (C) *SNAI1* expression in NTera2 cells. (D) *CYP24A1* expression in NTera2 cells. (E) *OCT4* expression in TCam-2 cells. (F) *NANOG* expression in TCam-2 cells. Expression is normalized to β2M and expression level at day 0. Values represent mean ± SD. All experiments are conducted in triplicates and have been repeated twice. Note different scales.

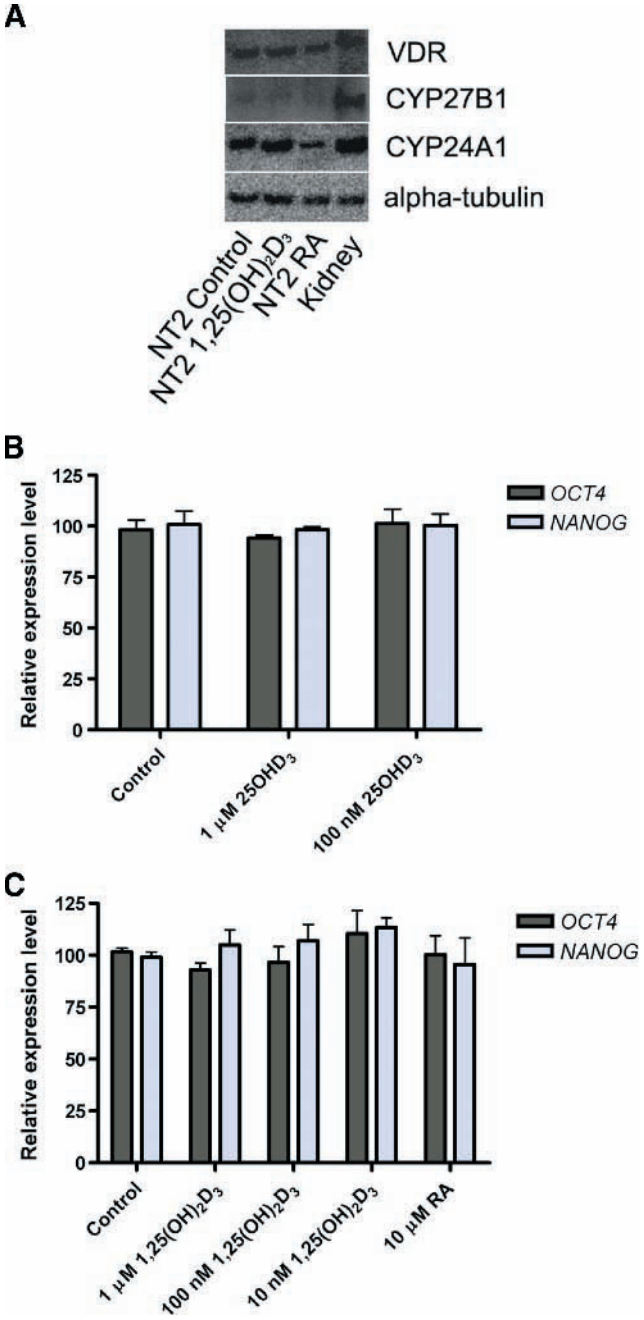

Figure W5. Gene and protein expression in NTera2 and 2102Ep cells. (A) WB of VDR, CYP27B1, CYP24A1, and α-tubulin following treatment with DMSO (control), 1 μM $1,25(OH)_2D_3$, or 10 μM RA in NTera2 cells and human kidney tissue used as positive control. (B) NTera2 cells treated with $25(OH)D_3$. (C) 2102Ep treated with $1,25(OH)_2D_3$ and RA. Expression is normalized to β2M and expression level at day 0. Values represent mean ± SD. All experiments are conducted in triplicates and have been repeated twice.